Fig. 2b that the pressure distribution is not self-similar for all pressure ratios. The observed merging of the profiles near the outlet is due to the boundary condition imposed at the duct exit. The lack of self-similarity in the ESJ can be explained by the presence of screech tones and their interactions. The jet behavior changes with the pressure ratio because the mixing characteristics are controlled by these interactions. For a single rectangular-jet ejector, the schlieren pictures of Hsia[2] and those taken in this study show this clearly. However, for the case of the multiple underexpanded jet, no such dominant discrete tones could be found.

Figures 3a and 3b show the self-similarity previously discussed for the case of the multiple-jet ejector for $AR = 26{:}1$ and 33:1. Results similar to those seen in Fig. 2b were obtained for the ESJ ejector at $AR = 26{:}1$ and 33:1, and these are presented and discussed in Chandrasekhara et al.[3]

Furthermore, the self-similarity is present only for short ejector nozzle to throat distances. At a large distance (5.2 cm), a clear breakdown can be seen (Fig. 4), even for $AR = 20{:}1$. This is because the jets tend to behave like freejets near the nozzle exit and generate discrete tones.

Conclusions

The wall static pressure distribution of a multiple underexpanded jet ejector scales well with the average throat static pressure. This is due to the absence of the well-defined acoustic interaction generally observed in the single underexpanded jet. The self-similarity obtained is for short nozzle to throat distances only.

Acknowledgment

This work was supported by the Air Force Office of Scientific Research under Contract F49620-79-0189. The authors appreciate the assistance of Ms. Pam Williams in the preparation of the original manuscript.

References

[1]Quinn, B., "Ejector Performance at High Temperatures and Pressures," *Journal of Aircraft*, Vol. 13, 1976, pp. 948–954.

[2]Hsia, Y.C., "An Experimental Investigation of an Underexpanded Rectangular Jet Ejector," Ph.D. Thesis, Dept. of Aeronautics and Astronautics, Stanford Univ., CA, March 1984.

[3]Chandrasekhara, M.S., Krothapalli, A., and Baganoff, D., "Mixing Characteristics of an Underexpanded Multiple Jet Ejector," JIAA TR-55, Stanford Univ., CA, June 1984.

Buckling of Shear-Deformable Plates

N. R. Senthilnathan,* S. P. Lim,† K. H. Lee,† and S. T. Chow‡
National University of Singapore, Singapore

Introduction

DESPITE the analytic simplicity, Kirchhoff's theory of plates cannot be employed reliably to analyze plates where shear deformation is known to have a significant effect. Reissner[1] was the first to present a shear-deformation theory of plates. Mindlin[2] presented a first-order theory of plates where he accounted for shear deformation in conjunction with a shear-correction factor. The present theory is obtained from Reddy's theory[3] using the assumption that the in-plane rotation tensor through the thickness is constant. The critical buckling loads obtained for isotropic, orthotropic, and composite laminates using the present theory agree very well with the results presented by Reddy and Phan.[4]

Many higher-order theories were also presented which include the effect of shear deformation directly by incorporating the higher-order terms in the displacement functions (for example, see Refs. 5 and 6). A fully three-dimensional theory of plates,[7] and a simple theory for plate bending[8] has also been given. All these theories involve many variables. Reddy[3] recently presented a simple higher-order theory of plates with five variables. This was done by neglecting transverse normal strain and imposing zero transverse shear strains at the two free surfaces using the theory of Lo et al. In the present paper, further simplifying assumptions given by 1) $w = w^b + w^s$, where w is the transverse displacement of the midplane plane and w^b and w^s are its components due to bending and shear, respectively, and 2) $\phi_n = -\nabla w^b$ where ϕ_n is the rotation vector, are made to Reddy's theory so that the number of variables is reduced by one. These assumptions imply that the in-plane rotation tensor is constant through the thickness and will be shown to have little effect on the critical buckling loads obtained for isotropic, orthotropic, and composite laminates. It is interesting to note certain common features between the present theory and the theories by Bhashyam and Gallagher[9] and by KrishnaMurty.[10] Bhashyam and Gallagher used the assumption $w = w^b + w^s$ in conjunction with Mindlin's theory. Thus, they had to introduce a shear correction factor. KrishnaMurty's theory also employed the same assumption but has one variable more than that of Reddy's theory.

Theory

Displacements

The displacement functions by Reddy[3] are given as

$$u = u_0 + z\left[\phi_x - \frac{4z^2}{3h^2}\left(\frac{\partial w}{\partial x} + \phi_x\right)\right]$$

$$v = v_0 + z\left[\phi_y - \frac{4z^2}{3h^2}\left(\frac{\partial w}{\partial y} + \phi_y\right)\right] \qquad w = w_0 \tag{1}$$

where u_0, v_0, and w_0 are the in-plane and transverse displacements at the midplane, ϕ_x and ϕ_y are the rotations of the normals to the cross sections, h and plate thickness, and z the coordinate in the tranverse direction. By making further assumptions given by

$$w_0 = w^b + w^s \qquad \phi_x = -w,_x^b \text{ and } \phi_y = -w,_y^b \tag{2}$$

It is seen that the functions given by Eq. (1) now take the simpler form

$$u = u_0 - z\frac{\partial w^b}{\partial x} - \frac{4z^3}{3h^2}\frac{\partial w^s}{\partial x}$$

$$v = v_0 - z\frac{\partial w^b}{\partial y} - \frac{4z^3}{3h^2}\frac{\partial w^s}{\partial y} \qquad w = w^b + w^s \tag{3}$$

Received June 30, 1986; revision received Jan. 26, 1987.

*Graduate Student, Department of Mechanical and Production Engineering.

†Lecturer, Department of Mechanical and Production Engineering.

‡Professor, Department of Mechanical and Production Engineering.

Table 1 Critical buckling loads $\lambda_c = N_1 b^2/\pi^2 D$, for isotropic ($\nu = 0.3$) rectangular plates under uniaxial compression

a/b	0.2(27.040)[a]		0.4(8.410)		1.0(4.000)		3.0(4.000)	
a/h	FSDPT[b]	Present HSDPT[c]	FSDPT	Present HSDPT	FSDPT	Present HSDPT	FSDPT	Present HSDPT
2	1.3988	1.6851	1.3761	1.4455	1.6597	1.6759	1.6597	1.6760
5	6.8753	7.0529	4.6264	4.6466	3.2626	3.2653	3.2636	3.2653
10	15.601	15.658	6.9824	3.9853	3.7864	3.7965	3.7864	3.7865
20	22.851	22.859	8.0010	8.0012	3.9443	3.9443	3.9443	3.9443
50	26.269	26.270	8.3417	8.3417	3.9903	3.9909	3.9909	3.9909
100	26.843	26.840	8.3928	8.3928	3.9977	3.9977	3.9977	3.9977

[a]Values within the parentheses indicate classical plate theory (CPT) values. [b]First-order shear deformation plate theory (from Ref. 4). [c]Higher-order shear deformation plate theory (from Ref. 4).

Table 2 Critical buckling loads $\lambda_c = (12N_1/\pi^2 E_1)(b/h)^2$, for homogeneous orthotropic square plates

h/b	CPT	Exact theory[7]	FSDPT[a] ($k = 5/6$)	HSDPT[a]	Present
0.05	3.039	2.966	2.9774	2.9774	2.9863
0.10	3.039	2.770	2.8074	2.8076	2.8394
0.20	3.039	2.210	2.2910	2.2933	2.3736

[a]Calculated using the expressions presented in Ref. 4.

Table 3 Critical buckling loads $\lambda_c = N_1 b^2/E_2 h^3$, for two-layered cross-ply square plates (0°/90°)

	(12.957)[a]		
a/h	FSDPT[b]	HSDPT[b]	Present
5	8.2772	8.7693	8.7693
10	11.3525	11.562	11.562
12.5	12.882	12.027	12.027
20	12.515	12.577	12.577
25	12.671	12.711	12.711
50	12.886	12.897	12.894
100	12.947	12.947	12.942

[a]CPT value. [b]Calculated using the expressions given in Ref. 4.

Table 4 Critical buckling loads $\lambda_c = N_1 b^2/E_2 h^3$, for two-layered angle-ply square plates (45°/−45°)

	(21.708)[a]		
a/h	FSDPT[b]	HSDPT[b]	Present
5	11.148	12.270	12.270
10	17.552	18.154	18.154
12.5	18.852	19.287	19.286
20	20.496	20.691	20.691
25	20.916	21.046	21.046
50	21.507	21.542	21.539
100	21.666	21.681	21.666

[a]CPT value. [b]Calculated using the expressions given in Ref. 4.

Strains

Following von Kármán assumptions for nonlinear strains, the strains can be expressed as

$$\epsilon_1 = \epsilon_{xx} = \frac{\partial u_0}{\partial x} + \frac{1}{2}\left(\frac{\partial w^b}{\partial x} + \frac{\partial w^s}{\partial x}\right)^2 - z\frac{\partial^2 w^b}{\partial x^2} - \frac{4z^3}{3h^2}\frac{\partial^2 w^s}{\partial x^2}$$

$$\epsilon_2 = \epsilon_{yy} = \frac{\partial v_0}{\partial y} + \frac{1}{2}\left(\frac{\partial w^b}{\partial y} + \frac{\partial w^b}{\partial y}\right)^2 - z\frac{\partial^2 w^b}{\partial y^2} - \frac{4z^3}{3h^2}\frac{\partial^2 w^s}{\partial y^2} \qquad \epsilon_3 = \epsilon_{zz} = 0$$

$$\epsilon_4 = 2\epsilon_{yz} = \left(1 - \frac{4z^2}{h^2}\right)\frac{\partial w^s}{\partial y} \qquad \epsilon_5 = 2\epsilon_{zx} = \left(1 - \frac{4z^2}{h^2}\right)\frac{\partial w^s}{\partial x}$$

$$\epsilon_6 = 2\epsilon_{xy} = \left(\frac{\partial w_0}{\partial y} + \frac{\partial v_0}{\partial x}\right) + \left(\frac{\partial w^b}{\partial x} + \frac{\partial w^s}{\partial x}\right)\left(\frac{\partial w^b}{\partial y} + \frac{\partial w^s}{\partial y}\right) - 2z\frac{\partial^2 w^b}{\partial x \partial y} - \frac{8z^3}{3h^2}\frac{\partial^2 w^s}{\partial x \partial y} \tag{4}$$

Governing Equations and Boundary Conditions

Using the strains given by Eqs. (4) in the virtual work principle with u_0, v_0, w^b, and w^s as variables and q as the applied load, the following equations are obtained

$$\delta u_0: \quad \frac{\partial N_1}{\partial x} + \frac{\partial N_6}{\partial y} = 0 \qquad \delta v_0: \quad \frac{\partial N_6}{\partial x} + \frac{\partial N_2}{\partial y} = 0$$

$$\delta w^b: \quad \left(\frac{\partial^2 M_1}{\partial x^2} + 2\frac{\partial^2 M_6}{\partial x \partial y} + \frac{\partial^2 M_2}{\partial y^2}\right) - f + q = 0$$

$$\delta w^s: \quad \frac{4}{3h^2}\left(\frac{\partial^2 P_1}{\partial x^2} + 2\frac{\partial^2 P_6}{\partial x \partial y} + \frac{\partial^2 P_2}{\partial y^2}\right) + \left(\frac{\partial Q_1}{\partial x} + \frac{\partial Q_2}{\partial y}\right) - \frac{4}{h^2}\left(\frac{\partial R_1}{\partial x} + \frac{\partial R_2}{\partial y}\right) - f + q = 0 \tag{5}$$

where

$$f = \frac{\partial}{\partial x}\left[N_1\left(\frac{\partial w^b}{\partial x} + \frac{\partial w^s}{\partial x}\right)\right] + \frac{\partial}{\partial y}\left[N_6\left(\frac{\partial w^b}{\partial x} + \frac{\partial w^s}{\partial x}\right)\right] + \frac{\partial}{\partial x}\left[N_6\left(\frac{\partial w^b}{\partial y} + \frac{\partial w^s}{\partial y}\right)\right] + \frac{\partial}{\partial y}\left[N_2\left(\frac{\partial w^b}{\partial y} + \frac{\partial w^s}{\partial y}\right)\right]$$

The boundary conditions are:

$$(un_x + vn_y) \text{ or } N_n \qquad (-un_y + vn_x) \text{ or } N_{ns}$$

$$w^b \text{ or } \left(\frac{\partial M_n}{\partial n} + 2\frac{\partial M_{ns}}{\partial s}\right) + \left(N_n\frac{\partial w^b}{\partial n} + N_{ns}\frac{\partial w^b}{\partial s}\right)$$

$$w^s \text{ or } Q_n + \frac{4}{3h^2}\left(\frac{\partial P_n}{\partial n} + 2\frac{\partial P_{ns}}{\partial s} - 3R_n\right) + \left(N_n\frac{\partial w^s}{\partial n} + N_{ns}\frac{\partial w^s}{\partial s}\right)$$

$$\frac{\partial w^b}{\partial n} \text{ or } M_n \qquad \text{and} \qquad \frac{\partial w^s}{\partial n} \text{ or } \left(\frac{4}{3h^2}\right)P_n \tag{6}$$

where

$$(N_i,M_i,P_i)=\int_{-h/2}^{h/2}\sigma_i(1,z,z^3)\mathrm{d}z \quad (i=1,2,6)$$

$$(Q_1,R_1)=\int_{-h/2}^{h/2}\sigma_5(1,z^2)\mathrm{d}z \quad (Q_2,R_2)=\int_{-h/2}^{h/2}\sigma_4(1,z^2)\mathrm{d}z \tag{7a}$$

and

$$N_n=N_1n_x^2+2N_6n_xn_y+N_2n_y^2$$

$$N_{ns}=(N_2-N_1)n_xn_y+N_6(n_x^2-n_y^2)$$

$$Q_n=Q_1n_x+Q_2n_y, \qquad R_n=R_1n_x+R_2n_y \tag{7b}$$

The components of the outward unit normal to the plate boundary in the x and y directions are n_x and n_y, respectively. M_n, M_{ns}, P_n, and P_{ns} are of the same form as N_n and N_{ns}.

Constitutive Equations

The stress resultants are related to the displacements by the following constitutive equations:

$$\{N_1'\}=[C_1]\{U_1\} \qquad \{N_2'\}=[C_2]\{U_2\} \tag{8}$$

where

$$\{N_1'\}^T=[N_1,N_2,N_6,M_1,M_2,M_6,P_1,P_2,P_6],$$

$$\{U_1\}^T=[u_{o,x},v_{o,x},(u_{o,y}+v_{o,x}),-w^b_{,xx},-w^b_{,yy},-2w^b_{,xy},$$

$$-(4/3h^2)w^s_{,xx},-(4/3h^2)w^s_{,yy},-(8/3h^2)w^s_{,xy}]$$

$$\{N_2'\}^T=[Q_1,Q_2,R_1,R_2]$$

and

$$\{U_2\}^T=[w^s_{,x},w^s_{,y},(-4/h^2)w^s_{,x},(-4/h^2)w^3_{,y}]$$

The transposed matrix is denoted by T.

Numerical Results

Exact Solutions for Simply Supported Plates

Critical buckling loads for simply supported isotropic, orthotropic, and composite laminates are obtained and compared with the results obtained using the theory of Reddy and Phan[4] and three-dimensional results[7] where available. The plate is subjected to an in-plane compressive load N_1 along the edges $x=0$ and a.

Exact solutions of the governing equations [Eqs. (5)] can be obtained for a simply supported plate with the boundary conditions

$$u(x,0)=u(x,b)=v(0,y)=v(a,y)=0$$

$$N_2(x,0)=N_2(x,b)=N_1(0,y)=N_1(a,y)=0 \quad \text{cross-ply} \tag{9a}$$

$$u(0,y)=u(a,y)=v(x,0)=v(x,b)=0$$

$$N_6(0,y)=N_6(a,y)=N_6(x,0)=N_6(x,b)=0 \quad \text{angle-ply} \tag{9b}$$

$$w^b=w^s=0 \text{ along the edges}$$

$$M_2(x,0)=M_2(x,b)=M_1(0,y)=M_1(a,y)=0$$

$$P_2(x,0)=P_2(x,b)=P_1(0,y)=P_1(a,y)=0 \tag{9c}$$

The following displacement functions which satisfy the above boundary conditions a priori are chosen:

$$u=\Sigma\Sigma u_{mn}\cos\alpha x\sin\beta y, \qquad v=\Sigma\Sigma v_{mn}\sin\alpha x\cos\beta y$$

for cross-ply laminates (10a)

$$u=\Sigma\Sigma u_{mn}\sin\alpha x\cos\beta y, \qquad v=\Sigma\Sigma v_{mn}\cos\alpha x\sin\beta y$$

for antisymmetric angle-ply laminates (10b)

$$w^b=\Sigma\Sigma w^b_{mn}\sin\alpha x\sin\beta y, \qquad w^s=\Sigma\Sigma w^s_{mn}\sin\alpha x\sin\beta y \tag{10c}$$

where $\alpha=m\pi/a$ and $\beta=n\pi/b$, a and b are the edge lengths of the plate along x and y axes, respectively, with thickness h. Using Eqs. (9) and (10) in the governing equations [Eqs. (5)], the following set of equations are obtained:

$$[[C]-\lambda[G]]\{\Delta\}=\{0\} \tag{11}$$

where $\{\Delta\}^T=[u_{mn},v_{mn},w^b_{mn},w^s_{mn}]$ and λ is the coefficient of the buckling load.

The results of critical buckling loads for rectangular isotropic plates with Poisson ratio $\nu=0.3$, and the results obtained by Reddy and Phan[4] are presented in Table 1. The two results are identical for all a/b and a/h ratios.

Table 2 shows a comparison of the buckling loads obtained by the present theory and the theory by Reddy and Phan,[4] with the three-dimensional results given by Srinivas and Rao[7] for an orthotropic plate. The results for the theory of Ref. 4 are obtained independently. The maximum difference between the two results for this case is about 3.5% for $h/a=0.2$. However, this difference is negligible when compared with the 37.5% difference between the three-dimensional and classical plate theory (CPT) values for the same h/a ratio. The elastic constants used in this case (as given in Ref. 7) are: $C_{22}/C_{11}=0.543103$, $C_{33}/C_{11}=0.530172$, $C_{12}/C_{11}=0.23319$, $C_{13}/C_{11}=0.010776$, $C_{23}/C_{11}=0.098276$, $C_{66}/C_{11}=0.262931$, $C_{55}/C_{11}=0.159914$, and $C_{44}/C_{11}=0.26681$, where C_{ij} is defined by $\sigma_i=C_{ij}\epsilon_i$ for $i,j=1,2,\ldots,6$. $i,j=1,2,\ldots,6$.

Tables 3 and 4 show the critical buckling loads for two-layered cross-ply and angle-ply (45°/−45°) laminates. Here also the results obtained by the theory and those obtained using the theory presented in Ref. 4 are in excellent agreement. The elastic constants used in the above case are: $E_1/E_2=40$, $G_{23}=0.5E_2$, $G_{12}=G_{13}=0.6E_2$, and $\nu_{12}=0.25$. The subscripts 1, 2, and 3 refer to the x, y, and z axes of the plates.

Conclusion

A simple shear deformation theory of plates is derived by making simplifying assumptions in Reddy's[3] theory. A comparison of the critical buckling loads obtained by the present theory with those obtained using Reddy's and three-dimensional theories, suggests that these assumptions have minimal effect on the accuracy of the results for the problems considered.

References

[1]Reissner, E., "The Effect of Transverse Shear Deformation on the Bending of Elastic Plates," *Journal of Applied Mechanics*, Vol. 12, 1945, pp. 69–77.

[2]Mindlin, R. D., "Influence of Rotatory Inertia and Shear on Flexural Motions of Isotropic, Elastic Plates," *Journal of Applied Mechanics*, Vol. 18, 1951, pp. 31–38.

[3]Reddy, J. N., "A Simple Higher-Order Theory for Laminated Composite Plates," *Journal of Applied Mechanics*, Vol. 51, No. 4, 1984, pp. 745–752.

[4]Reddy, J. N. and Phan, N. D., "Stability and Vibration of Isotropic, Orthotropic and Laminated Plates According to a Higher-

Order Shear Deformation Theory," *Journal of Sound and Vibration*, Vol. 98, No. 2, 1985, pp. 157-170.

[5]Nelson, R. B. and Lorch, D. R., "A Refined Theory for Laminated Orthotropic Plates," *Journal of Applied Mechancis*, Vol. 41, 1974, pp. 177-183.

[6]Lo, K. H., Christensen, R. M., and Wu, E. M., "A Higher-Order Theory of Plate Deformation, Part 1: Homogeneous Plates," *Journal of Applied Mechanics*, Vol. 44, 1977, pp. 663-668.

[7]Srinivas, S. and Rao, A. K., "Bending, Vibration and Buckling of Simply Supported Thick Orthotropic Rectangular Plates and Laminates," *International Journal of Solids and Structures*, Vol. 6, 1970, pp. 1463-1481.

[8]Rehfield, L. W. and Rao, V. R., "A Simple, Refined Theory for Bending and Stretching of Homogeneous Plates," *AIAA Journal*, Vol. 22, Jan. 1984, pp. 90-95.

[9]Bhashyam, G. R. and Gallagher, R. H., "An Approach to the Inclusion of Transverse Shear Deformation in Finite Element Plate Bending Analysis," *Computers and Structures*, Vol. 19, No. 1-2, 1984, pp. 35-40.

[10]KrishnaMurty, A. V., "Toward a Consistent Plate Theory," *AIAA Journal*, to be published.

[11]Jones, R. M., *Mechanics of Composite Materials*, Scripta Book Co., Washington, DC, 1975.

Temperature Variation of the Elastic Constants of Aluminum Alloy 2090-T81

J. Glazer* and J. W. Morris Jr.†
Lawrence Berkeley Laboratory
University of California Berkeley, California

and

S. A. Kim,‡ M. W. Austin,‡ and H. M. Ledbetter§
National Bureau of Standards, Boulder, Colorado

ALUMINUM is often the material of choice for weight-critical structures used at cryogenic temperatures. Current aerospace applications include the external tank of the space shuttle, currently manufactured from aluminum alloy 2219. Future applications might include tanks for proposed hypersonic vehicles. Aluminum-lithium alloys have been proposed for these applications because they provide mechanical properties comparable or superior to those of existing aerospace aluminum alloys at 7-10% lower density and higher stiffness. Since stiffness is an important design criterion for structures like tanks, the elastic constants for these materials at low temperature are important design properties. This Note focuses on a particular aluminum-lithium alloy that may see cryogenic service, namely alloy 2090-T81.

Aluminum-lithium alloys of commercial compositions have elastic moduli at room temperature approximately 7-12% higher than those of conventional aluminum alloys. The increase in elastic modulus is related primarily to the amount of lithium in the alloy, so it can vary significantly even within the specified composition ranges of commercial alloys.[1,2] The temperature variation of the elastic constants of various commerical aluminum alloys has been studied previously.[3,4] All aluminum alloys behave similarly, displaying an increase in elastic modulus of about 12% between room temperature and 4 K. This Note confirms this trend for the aluminum-lithium alloy 2090-T81. Titanium alloys, which are also used for cryogenic tanks, show a smaller increase in stiffness at low temperatures.[4]

The alloy studied in this investigation, 2090-T81, has a nominal chemical composition of Al-2.7Cu-2.2Li-0.12Zr in weight percent. The chemical composition limits and the actual chemical composition, as determined by atomic absorption spectroscopy, are given in Table 1. In longitudinal and transverse orientations, this alloy shows improved strength, elongation, and fracture toughness at low temperatures. The mechanical properties at 298 K, 77 K, and 4 K are given in Ref. 5. The elastic-constant measurements were performed using ultrasonic (10 MHz) pulse techniques. The experimental procedure is described in detail elsewhere.[4,6] Except for high-strain cases, dynamic elastic constants equal static-elastic constants within the usual uncertainty of the latter. For the dynamic values, we estimate the uncertainty as 0.1%. Static and dynamic values should show essentially identical temperature behavior.

Figure 1 shows the Young's modulus and Poisson's ratio of 2090-T81 alloy as a function of temperature between 295 K and 4 K. The values at selected temperatures are listed in Table 2. The room-temperature value of the Young's modulus lies close to the reported average values from static tensile tests.[2] The temperature variation is similar to that observed for other aluminum alloys.[4]

Table 1 Chemical composition limits for 2090 alloy and actual composition of the material used in this study

Element	Al	Cu	Li	Zr	Fe
Composition limits	Balance	2.4-3.0	1.9-2.6	0.08-0.15	0.10
Actual composition	Balance	2.86	2.05	0.12	0.02

Element	Si	Mg	Mn	Ti
Composition limits	0.12	0.25	0.05	0.15
Actual composition	<0.01	<0.01	<0.005	0.02

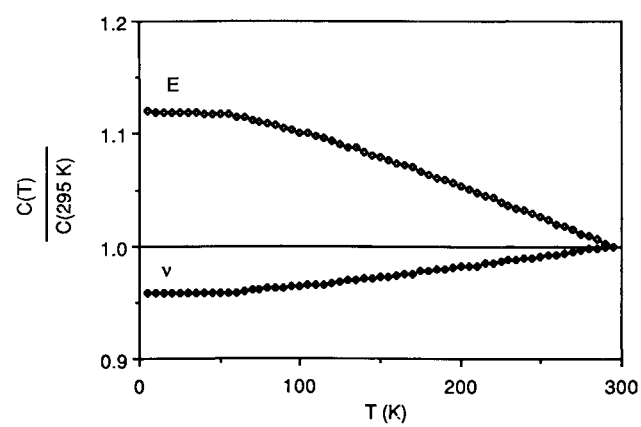

Fig. 1 Young's modulus (E) and Poisson's ratio (ν) of 2090-T81 alloy as functions of temperature. The plotted values are ratios between the actual values and the room-temperature values given in Table 2.

Received Dec. 3, 1986.

*Graduate Student.

†Structural Materials Group Leader, Center for Advanced Materials, and Professor of Metallurgy, Department of Materials Science and Mineral Engineering.

‡Reseach Engineer, Fracture and Deformation Division, Institute for Materials Science and Engineering.

§Metallurgist, Fracture and Deformation Division, Institute for Materials Science and Engineering.